Available online at www.sciencedirect.com
SCIENCE DIRECT®
International Journal of Pharmaceutics 252 (2003) 87–98
international journal of pharmaceutics
www.elsevier.com/locate/ijpharm

Influence of physico-chemical carrier properties on the in vitro aerosol deposition from interactive mixtures

Margaret D. Louey[1], Sultana Razia, Peter J. Stewart*

Department of Pharmaceutics, Victorian College of Pharmacy, Monash University, Parkville, Vic., Australia

Received 6 July 2002; received in revised form 15 November 2002; accepted 15 November 2002

Abstract

Interactive mixtures were prepared containing 5% (w/w) salbutamol sulfate using various lactose carrier systems, including sieved fractions and blended mixtures of coarse and fine particles. The solid state and powder properties of the lactose carriers were examined by laser diffraction, differential scanning calorimetry, thermogravimetric analysis, powder X-ray diffraction, vapor sorption gravimetry, rotating drum and atomic force microscopy. The in vitro aerosol deposition was determined using a twin-stage impinger with a Rotahaler at an airflow rate of 60 l/min. The fine particle fraction (FPF) of salbutamol sulfate was determined using a validated HPLC assay. All samples were highly crystalline with minimal moisture sorption and the major phase in all samples was α-lactose monohydrate. Significant differences in FPF were observed using the various carrier systems. FPF increased with decreasing carrier $d_{50\%}$ ($r^2 = 0.919$) and increasing proportion of fine carrier particles (below 5 μm) ($r^2 = 0.841$). Carriers consisting of very large proportions of fine particles showed low FPF and did not fit the correlation. The presence of coarse carrier particle fractions was essential to achieve maximum FPF, which occurred when about 10% of fine carrier particles were present in the mixture. Dispersion characteristics may be related to the degree of drug aggregation on the carrier surface.

Keywords: Lactose; Salbutamol sulfate; Dry powder inhalers; In vitro aerosol deposition; Atomic force microscopy

1. Introduction

Dry powder inhaler (DPI) formulations require drug particles with aerodynamic diameters below 5 μm for lung deposition and good flow properties to ensure accurate dose metering of the drug and ease of manufacturing processes. A formulation strategy used to fulfil both requirements includes the use of interactive mixtures (previously known as ordered mixtures, Hersey, 1975), which consist of micronized drug particles adhered to the surface of larger carrier particles. Redispersion of the drug particles from interactive mixtures is required for a respirable lung deposition (Ganderton, 1992). The degree of drug redispersion depends upon the forces of interaction within the powder formulation and the mechanical forces of dispersion from the device and patient's inspiration. Strong interparticulate forces within the powder formulation may lead to poor efficiency (Byron, 1986). Low efficiency has been observed in commercial DPI products, producing a fine particle dose of 20-30% of the total emitted dose at 60 l/min (Steckel and Müller, 1997). Factors affecting

* Corresponding author. Tel.: +61-3-9903-9517; fax: +61-3-9903-9583.
E-mail address: peter.stewart@vcp.monash.edu.au (P.J. Stewart).
[1] Present address: Inhalation Product Development, GlaxoSmithKline, Research Triangle Park, NC, USA.

0378-5173/02/$ – see front matter © 2002 Elsevier Science B.V. All rights reserved.
PII: S0378-5173(02)00621-X

interparticulate forces within the powder formulation include the drug and carrier properties, drug-carrier ratio, ternary components, mixing process conditions and storage conditions (Ganderton, 1992).

Particle adhesion may be affected by the physico-chemical properties of carrier particles, such as particle size distribution, surface roughness, crystallinity, elastic/plastic deformity, electrostatic behavior and moisture sorption. Although some investigations on the effect of carrier properties on the in vitro aerosol deposition of DPI formulation have been undertaken, many conflicting reports exist.

Recrystallized lactose carriers with low surface roughness (rugosity) produced higher deposition of salbutamol sulfate by facilitating more effective redispersion (Kassem and Ganderton, 1990). In contrast, lactose carriers with microscopic surface roughness produced higher deposition of pranlukast hydrate than carriers with smooth or macroscopically rough surfaces (Kawashima et al., 1998). This was attributed to reduced adhesion due to smaller interparticulate contact area. No direct relationship was observed between lactose carrier shape and surface roughness and the mass median aerodynamic diameter (MMAD) of salmeterol xinafoate from powder mixtures (Podczeck, 1998).

Higher drug deposition has been observed with smaller carrier sizes in a number of studies. Increased respirable fractions of salbutamol sulfate were observed with decreasing lactose carrier size (Kassem et al., 1989). Increased fine particle fractions (FPF) of disodium cromoglycate (DSCG) were observed with smaller carrier sizes of lactose and glucose (Braun et al., 1996). Decreased FPF of budesonide was obtained from increased lactose carrier sizes (Steckel and Müller, 1997). Decreased respirable fraction of mannitol and mannitol-recombinant human granulocyte-colony stimulating factor occurred with increasing PEG carrier size (French et al., 1996). However, differences in FPF of rhDNase were not observed with carrier type or size (Chan et al., 1997). Also, no relationship was observed between lactose carrier size and MMAD of salmeterol xinafoate (Podczeck, 1998).

The proportion of fine carrier particles has been observed to affect drug deposition. Higher respirable fractions of salmeterol xinofoate were obtained a lactose carrier with a higher proportion of fine particles even though the same sieve fraction (63–90 μm) was used (Mackin, et al, 1997). Higher FPF of salbutamol sulfate (SS) was obtained from the mixture containing a micronized lactose carrier compared to Lactochem (20.10 μm) (Srichana et al., 1998). However, increased proportion of fine lactose carrier particles increased the MMAD of salmeterol xinafoate (Podczeck, 1998).

The objective of this paper was to indentify the critical physico-chemical properties of lactose-carrier particles that influenced the in vitro aerosol deposition of binary interactive mixtures using salbutamol sulfate as the model drug. Lactose was chosen as the carrier since it is the only excipient approved for use in inhalation therapy and a range of lactose carrier systems were chosen or developed from readily available samples. Solid state crystalline characteristics were determined using thermal analysis, X-ray crystallography and water adsorption methods. Particle size distributions, powder flow properties and particle adhesion were used to characterize the powder properties of the carrier systems.

2. Materials and methods

2.1. Materials

Micronized salbutamol sulfate (SS; Glaxo Wellcome, Australia; Lot 700274; $d_{10\%}$, $d_{50\%}$ and $d_{90\%}$ = 0.7, 1.3 and 2.9 μm, respectively) was employed as the model drug for preparation of binary interactive mixtures. Ten different grades of lactose (three manufacturers) were employed: Microfine (MF; Borcula Whey Products Ltd., UK); Superfine (SF), 100 Mesh (100 M), Special Dense (Sp D) and Edible (Ed; New Zealand Milk Products Pty. Ltd., Australia); and Pharmatose DCL11 (DCL11), Pharmatose 110 Mesh (110 M), Pharmatose 125 Mesh (125 M), Pharmatose 325 Mesh (325 M) and Pharmatose 450 Mesh (450 M) (DMV International, The Netherlands). The lactose carriers were used as received. 325 M was designated as the control carrier for physico-chemical and aerosol studies as it is the only inhalation-grade lactose used. In addition, sieved sized fractions of the Edible carrier were prepared using test sieves and a sieve shaker (Labtechnics, Australia) where a 200 g load was shaken for 20 min. The sieved size fractions used include: smaller than 63, 63–90, 90–125,

125–150 and 150–212 μm. Edible carrier was chosen for size fractionation as it provided the large size distribution required for the size ranges obtained.

2.2. Physico-chemical characterization of lactose carriers

2.2.1. Particle size analysis

Particle size distributions were determined using laser diffraction (Malvern Mastersizer S, Malvern Instruments, UK) in a magnetically stirred cell with ethanol as the liquid dispersant (300 mm Fourier lens, 14.3 mm active beam length and background correction). Samples were sonicated for 3 min immediately prior to measurement. The mean particle size distribution of five replicates was determined. The size distributions were characterized using the diameters at the 10, 50 and 90 percentile ($d_{10\%}$, $d_{50\%}$ and $d_{90\%}$, respectively) and the percentage of particles below 5 μm.

2.2.2. Differential scanning calorimetry (DSC)

Thermal properties were analyzed using a differential scanning calorimeter (DSC; Model DSC7, Perkin-Elmer, CT), calibrated with indium (melting point of 156.6 °C) and lead (melting point of 327.47 °C), under a nitrogen gas purge. Samples (2–5 g) were crimp-sealed in 50 μl aluminium pans with pierced lids and analyzed in the range between 80–250 °C, using a heating rate of 5 °C/min with baseline correction. The onset temperatures and heat of enthalpy (ΔH) for each peak were determined from the normalized DSC thermogram.

2.2.3. Thermogravimetric analysis (TGA)

The weight loss on heating was analyzed by a thermogravimetric analyser (TGA; Model TGA7, Perkin-Elmer, CT) under a nitrogen purge. The samples (2–5 mg) were analyzed in platinum pans at the temperature range of 50–250 °C with a scanning rate of 5 °C/min. The weight loss on heating was expressed at a percentage of the initial weight.

2.2.4. Powder X-ray diffraction (PXRD)

Crystalline properties were examined using a X-ray diffractometer (Model PAD V, Scintag Inc., CA). Samples (2–5 mg) were placed in a quartz 'zero background' holder and measured using Cu Kα radiation with angular increments of $2\theta = 0.030^\circ$ in the range of 2–100°, with increments of 2°/min.

2.2.5. Vapor sorption gravimetry

Moisture sorption isotherms were determined using an automated vapor sorption analyser (Dynamic Vapor Sorption DVS.1, Surface Measurements Systems Ltd., UK). Measurements were performed at 20 °C, under a continuous nitrogen flow of 200 cm^3/min, using 50 mg samples in the range of 15–95%RH. The relative humidity was held at each 20%RH increment until equilibrium occurred (with a minimum time limit of 30 min and maximum of 60 min at each step). The sample mass was represented as a percentage of the initial mass.

2.2.6. Flowability

Powder flowability was characterized using a rotating powder drum (Aero-Flow, Amherst Process Instruments Inc., MA). Samples (100 g) were rotated at 60 rpm and the time intervals between avalanches were measured for 180 s, excluding the first avalanche time. The mean time to avalanche, standard deviation and number of avalanches were determined for each sample for the specified time period.

2.2.7. Adhesional properties

The adhesional force on the carrier surface were measured with an atomic force microscope (AFM) (Dimensions 3100, Digital Instruments, CA) using a colloid probe technique in air at room temperature (20–25 °C) and ambient humidity (40–50%RH). The colloid probe consisted of a 10 μm diameter silica sphere (Kunishima Kikai Ltd., Japan) attached to the apex of V-shaped silicon nitride cantilever (Type NP-S, Digital Instruments, CA) (cantilever spring constant, $k = 0.42$ N/m). Full details are provided elsewhere (Louey et al., 2001). Briefly, individual adhesion forces were measured between a colloid probe and the lactose carrier surface. The vertical displacement of the cantilever (pull-off distance) of each individual adhesion was determined from the force–distance plot using a software analysis program (AFM Analysis, Patrick Hartley, CSIRO, Australia). The individual adhesion forces were determined using Hooke's law, where the vertical cantilever displacement was multiplied with the cantilever spring constant.

The adhesion force distribution of each sample was obtained by adhesion measurements at greater than 50 individual sites on at least three different particles. Regression analysis was performed on the log-transformed adhesion data using a least-squares method (Minitab, Minitab Inc., PA). The geometric mean was determined from the adhesion force at which 50% of the population was distributed ($F_{50\%}$). The geometric standard deviation (GSD) was calculated from the ratio of $F_{50\%}$ to $F_{16\%}$, where $F_{16\%}$ represented the adhesion force at which 16% of the population was distributed.

Comparison between lactose samples was performed on the log-transformed data using either a Mann–Whitney rank sum test or Kruskal–Wallis one-way analysis of variance on ranks (Sigmastat, Jandel Scientific, CA) at the 5% significance level. Multiple comparison between groups was performed at the 5% significance level overall using the Dunn's test (Sigmastat, Jandel Scientific, CA).

2.3. Preparation of interactive mixtures

Interactive mixtures containing 2.5 and 5% (w/w) drug concentration were prepared in 5 g batches. Micronized SS was placed between two layers of lactose carrier (or lactose carrier mixed with micronized lactose) in a glass test-tube containing three ceramic beads (approximately 10 mm diameter) and shaken vigorously by hand for 5 min. The ceramic beads provided a ball-rolling effect for breaking up the drug agglomerates present. This mixing technique was modified from a previously used method (Alway et al., 1996). The order of mixing of the SS, micronized lactose and lactose carrier has been shown not to influence the dispersion Louey and Stewart, 2002).

2.4. Homogeneity

Twenty samples (150 mg), obtained by selecting small samples of powder by spatula from various locations in the container, were dissolved in 0.1 M hydrochloric acid and the amount of SS in each sample was determined by a validated UV assay at a wavelength of 276.2 nm (Cecil CE6600 UV spectrophotometer, UK). Linearity was achieved between 3 and 300 μg/ml, with the LOD and LOQ determined at 0.75 and 1.50 μg/ml, respectively. An acceptable degree of homogeneity was achieved with a mean drug content within 10% of the theoretical value and coefficient of variation (CV) less than 3% (Crooks and Ho, 1976). Homogeneity determinations using a more appropriate sample size of 20 mg were undertaken for a limited number of SS mixtures. The mean drug content was well within 10% of the theoretical value and all mixtures showed a CV below 4%.

2.5. In vitro aerosol deposition

In vitro aerosol deposition was determined using a twin-stage impinger (TSI; Copley, UK) with 7 and 30 ml purified water (Milli-Q, Millipore, MA) placed into stages 1 and 2, respectively. The airflow was drawn through the TSI using a vacuum pump (Dynavac Engineering, Australia). The airflow rate was adjusted to 60 l/min at the mouthpiece, prior to each measurement. The aerodynamic cut-off diameter at 60 l/min was 6.4 μm. The temperature and relative humidity of the surrounding environment was measured using a thermo-hygrometer (Shinyei TRH-CZ, Japan). Powder mixture (20 mg) was loaded into hard gelatin capsules (size 3, Fawns and McAllan Pty. Ltd., Australia). The Rotahaler (Glaxo Wellcome) was placed into a molded mouthpiece attached the TSI and an air volume of four litters was drawn for each measurement (4 s at 60 l/min). Each section (inhaler, stages 1 and 2) was rinsed with purified water. The rinsing liquid was collected and diluted to an appropriate volume.

The SS content was determined by a validated HPLC assay. A reverse phase HPLC method was used (Waters μBondapak; 125 Å, 10 μm, 3.9 mm × 300 mm, MA) with a flowrate of 1 ml/min and a wavelength of 276 nm (Waters Tunable Absorbance Detector, MA). The mobile phase consisted of a 2:1 (v/v) mixture of 0.2% (w/v) ammonium acetate and methanol, filtered and degassed immediately prior to use. An injection volume of 100 μl was used. The concentration of SS was determined from peak area using external aqueous standards, with linearity between 0.04 and 20 μg/ml. The LOQ and LOD were determined at 0.04 and 0.02 μg/ml, respectively.

TSI measurements were performed in replicates of five. The recovered dose was defined as the total amount of drug collected in the inhaler, stage 1 (S1)

and stage 2 (S2). The fine particle fraction (FPF) was defined as the amount of drug particles deposited in the lower stage of the TSI as a percentage of the amount of drug particles deposited in both stages (Eq. (1)).

$$\text{FPF}\ (\%) = \frac{S2}{S1 + S2} \times 100 \quad (1)$$

Comparison between TSI deposition data was performed using a one-way analysis of variance (ANOVA; Sigmastat) at a 5% significance level with multiple comparison was performed at the 5% level overall using a Tukey test (Sigmastat, Jandel Scientific, CA).

3. Results and discussion

3.1. Drug dispersion

The in vitro aerosol deposition studies were conducted in an air-conditioned laboratory, where the ambient temperature and relative humidity was $21 \pm 3\,^{\circ}\text{C}$ and $52 \pm 12\%$RH, respectively. The drug recovery ranged between 81.6 and 98.8%, which was within the acceptable range (75–125%) for mass balance (Byron et al., 1994). The fine particle fraction (FPF) obtained from the binary mixtures containing the different carrier types ranged from 3.4 to 39.1%, with significant differences observed due to carrier type (Fig. 1) ($P < 0.001$).

3.2. Solid state characterization of the carrier

All samples were highly crystalline. In the X-ray diffractogram, the major peaks of all lactose carriers were consistent with those of α-lactose monohydrate and the presence of β-lactose was not detected. Slight variations in peak intensity observed between samples were considered to be due to preferred orientation and minor differences in crystallinity. In the DSC studies, sharp transition endothermic peaks were observed at temperatures of 140, 210 and 220 °C and a broad endothermic peak was observed around 240 °C. A summary of onset temperatures, heat of enthalpies (ΔH) and weight losses on heating is presented in Table 1. The thermal analysis supported the presence of α-lactose monohydrate by the release of water

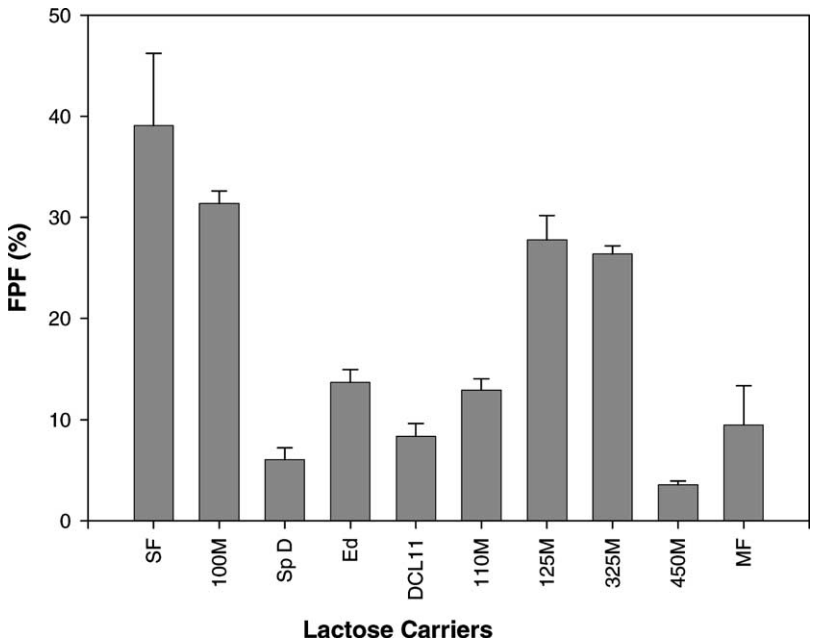

Fig. 1. The FPF of a 5% binary mixture containing different lactose carriers described in Section 2.1 (mean ± S.D., $n = 5$).

Table 1
Summary of thermal parameters of lactose carriers determined by DSC and TGA, using a heating rate of 5 °C/min

Lactose carrier	Peak 1			Peak 2		Peak 3	
	Onset (°C)	ΔH (J/g)	Weight loss (%)	Onset (°C)	ΔH (J/g)	Onset (°C)	ΔH (J/g)
SF	141.88	196.20	5.135	209.30	115.32	–	–
100 M	141.77	182.57	4.800	208.90	75.81	–	–
Sp D	142.25	134.40	4.697[a]		208.76	94.56	–
Edible	142.15	120.89	4.634[a]	211.82	111.53	–	–
DCL11	134.29	160.57	4.945	208.31	110.65	219.99	19.93
110 M	133.60	113.15	4.460	205.60	104.13	–	–
125 M	131.65	154.90	4.985	204.90	103.96	216.46	14.19
325 M	139.08	192.83	5.020	207.30	107.16	218.63	22.33
450 M	134.95	175.27	5.070	207.61	111.50	216.59	8.48
MF	145.06	197.86	4.775	208.93	106.34	–	–

[a] Determined using heating rate of 10 °C/min.

of crystallization at 140 °C and the melting peak of α-lactose anhydrous at 210 °C (Lerk et al., 1984). The accompanying weight loss of approximately 5% was representative of the stoichiometric weight of the hydrate water. The values for the enthalpy of dehydration ranged from 131.65 to 145.06 J/g, which was similar to those obtained in the literature (Angberg et al., 1991; Sebhatu et al., 1994). The peak observed at 220 °C in the DSC thermograms of DCL11, 125, 325 and 450 M samples was representative of the melting of β-lactose anhydrous (Lerk et al., 1984). However, the absence of β-lactose in the XRD data suggests that the β-lactose was a result of mutarotation during the thermal treatment. The broad peak observed around 240 °C was attributed to thermal degradation following melting. Charring was confirmed by visual examination at the end of the DSC run. The absence of an exothermic crystallization peak around 180 °C indicated very little amorphous content in the lactose samples.

The vapor sorption isotherms of the lactose carriers indicated that both amorphous content and moisture adsorption were minimal. The moisture adsorption mainly occurred at 95%RH. α-Lactose monohydrate is non-hygroscopic with moisture sorption occurring at 95%RH (Kibbe, 2000). The minimal weight gain, in the general order of 0.02%, obtained following the adsorption–desorption cycle suggested that a minimal amount of amorphous phase was present in the lactose samples. However, there was an absence of weight gain in the adsorption stage at the critical humidity (around 50%RH) where amorphous lactose crystallizes. The levels of amorphous material present in the lactose samples may be too low to be detected in this study. Levels of 0.05–0.5% amorphous lactose were previously observed using moisture vapor sorption (Buckton and Darcy, 1995).

3.3. Powder properties of the carrier

Significant differences were observed in powder flowability of lactose carriers (Table 2) ($P < 0.001$). Longer times to avalanche were observed for SF, 100,

Table 2
Summary of flowability data for lactose carriers determined using a rotating drum

Lactose carrier	Avalanche[a] time (s)	Standard deviation[a] (s)	Number of avalanches[b]
SF	3.7*	1.7	48
100M	2.6*	0.8	66
Sp D	2.0	0.8	89
Edible	2.1	0.7	86
DCL11	2.0	0.9	86
110 M	1.9	0.7	91
125 M	2.0	0.7	86
325 M	1.8	0.8	98
450 M	3.3*	1.4	52
MF	3.5*	1.6	51

[a] Excluding the first avalanche.
[b] For a period of 180 s.
* Represents a significant difference ($P < 0.05$) compared with 325 M (control).

450 M and MF carriers compared with 325 M (control), which were indicative of poorer flow properties. The poor flow observed for MF, 450 M and SF carriers was attributed to their small median size (<50 μm in each case) and the high proportion of fine particles smaller than 5 μm (Neumann, 1967; Staniforth, 1988). Since 100 M has a $d_{50\%}$ of 103.78 μm, the observed poor flow properties were unexpected. The reason for this was not further investigated. 100 M had better flow than MF, 450 M and SF carriers. Due to the manufacturing processes, MF and DCL11 had different surface morphology compared with the other carriers. There was little correlation observed between FPF and powder flowability (Fig. 2A) ($r^2 = 0.02$).

Significant differences have been observed in the adhesional properties of lactose carriers (Louey et al., 2000) using an atomic force microscopy (AFM) colloid probe technique ($P < 0.001$). The adhesional

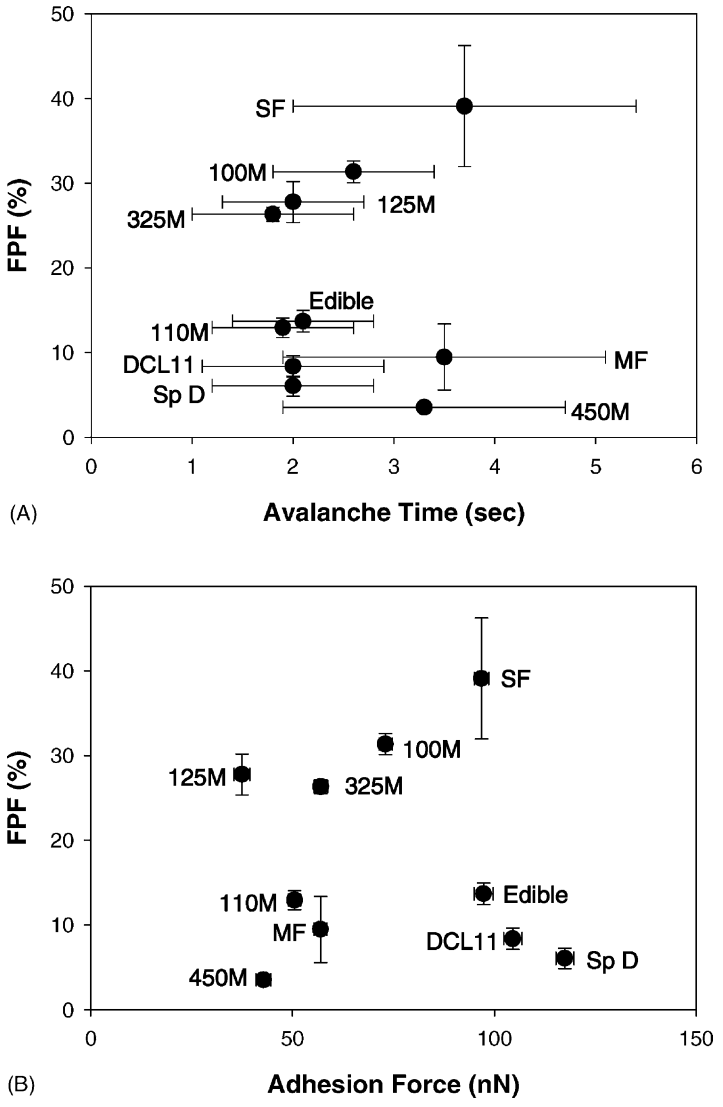

Fig. 2. Relationship between the FPF (mean ± S.D., $n = 5$) and (A) the flowability of the lactose carrier (mean ± S.D., $n > 48$), and (B) the adhesion force (nN) measured between using a 10 μm colloid probe (geometric mean ± S.D., $n > 50$).

force was measured between lactose surfaces and a silica sphere attached to the AFM cantilever using individual force distance curves. Higher adhesion was obtained from SF, Sp D, Edible and DCL11, compared with 325 M (control). Lower adhesion was obtained from 125 M, compared with 325 M (control). There was little correlation observed between FPF and adhesional properties of lactose carriers (Fig. 2B) ($r^2 = 0.005$). The AFM study provided a relative adhesional characterization of the lactose with respect to a standard silica sphere of known dimensions and geometry. Ideally, the determination of adhesion between the carrier and SS particle would be more appropriate; however, adhesional force determinations between the carrier and SS particle are problematic due to variable SS particle size, shape and friability giving rise to large errors in contact area and considerable variability in results.

Major differences were observed in the particle size distribution of the lactose carriers used in this research, with carrier median size ($d_{50\%}$) ranging from 4.0 to 190.8 μm (Table 3). The proportion of fine particles (below 5 μm) ranged from 0.6 to 60.5%.

A strong trend was observed where the FPF increased with reducing carrier $d_{50\%}$ ($r^2 = 0.712$) (Fig. 3A), apart from MF and 450 M carriers, both of which possessed few larger, non-cohesive particles. The apparent inverse relationship between carrier $d_{50\%}$ and FPF was confirmed by the excellent correlation ($r^2 = 0.919$) obtained using size fractions of the Edible carrier (Fig. 4A). Significant differences in FPF were observed with the different size fractions of Edible carrier size ($P < 0.001$). Size fractions smaller than 90 μm produced higher FPF ($P < 0.05$ each) compared with the non-size fractioned Edible carrier (control), whereas size fractions above 150 μm produced lower FPF ($P < 0.05$). These results were supportive of the increased FPF with decreasing carrier size observed in previous reports (Kassem et al., 1989; Braun et al., 1996; Steckel and Müller, 1997; French et al., 1996).

Apart from binary mixtures containing MF and 450 M carriers, a strong trend was observed between the FPF and the percentage of carrier particles below 5 μm ($r^2 = 0.640$) (Fig. 3B). A good correlation was observed using sieved size fractions of Edible carrier ($r^2 = 0.841$) (Fig. 4B). Increased FPF was produced with carriers containing a higher proportion of fine particles (below 5 μm), until a certain level. These results were similar to a previous finding where higher FPF was attributed to a higher proportion of fine carrier particles (Mackin et al., 1997).

The difference in behavior observed for MF and 450 M carriers may be due to their small carrier $d_{50\%}$ and high proportion of particles smaller than 5 μm causing agglomeration. Strong aggregation forces increase the “effective” particle size and reduce the proportion of fine particles. Since MF and 450 M carriers (carrier $d_{50\%}$ of 4.0 and 19.6 μm, respectively) were

Table 3
Particle size distribution of lactose carriers determined by laser diffraction (mean, $n = 5$)

Sample	$d_{10\%}$ (μm)	$d_{50\%}$ (μm)	$d_{90\%}$ (μm)	Size < μm (%)
SF	3.9	35.4	100.6	12.1
100 M	11.5	103.8	281.5	6.2
Sp D	62.3	176.5	346.6	2.5
Edible	24.6	190.8	480.4	4.3
Edible (size < 63 μm)	6.6	40.0	76.7	8.3
Edible (63–90 μm)	47.1	84.4	120.0	3.6
Edible (125–150 μm)	57.9	151.0	220.3	3.9
Edible (150–212 μm)	89.1	194.6	290.5	3.4
DCL11	58.2	124.8	227.0	0.6
110 M	75.1	148.1	255.6	1.0
125 M	25.8	67.2	121.8	2.8
325 M	5.0	54.3	95.9	10.0
450 M	3.5	19.5	45.6	13.6
MF	1.1	4.0	9.0	60.5

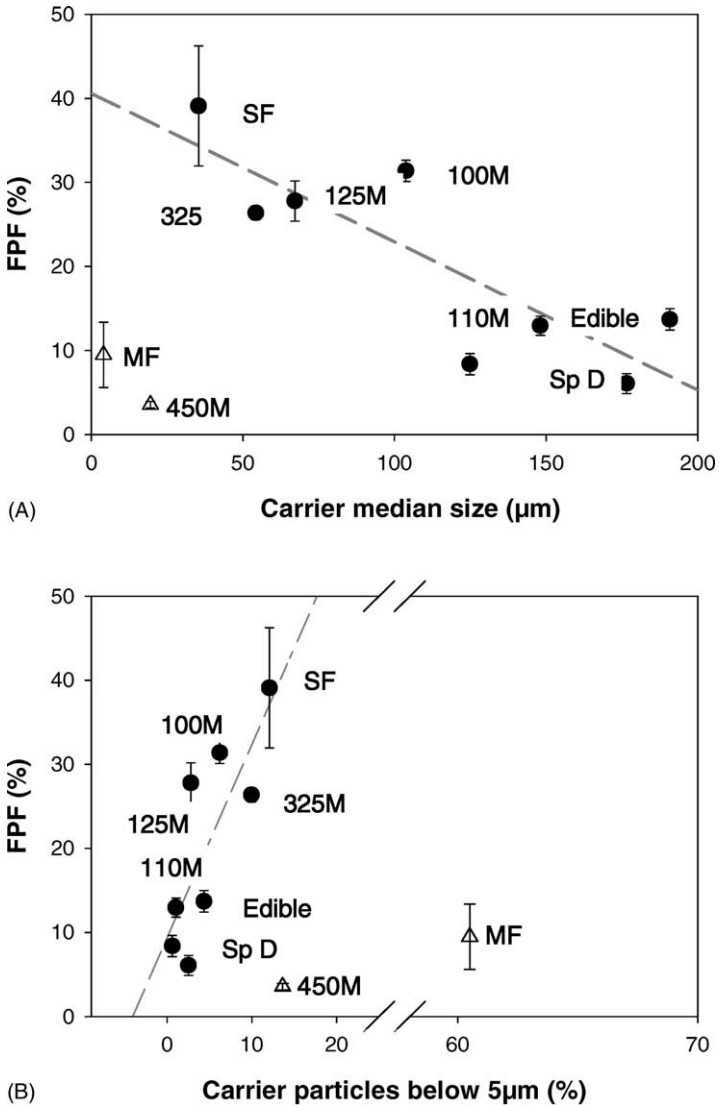

Fig. 3. Relationship between the FPF (mean ± S.D., $n = 5$) and (A) the carrier median diameter (regression coefficient, $r^2 = 0.71$) and (B) the proportion of carrier particles below 5 μm (regression coefficient, $r^2 = 0.64$) using 10 lactose carriers.

considerably smaller than the other carriers, it may be possible that drug-fine carrier aggregates were produced instead of interactive mixtures, which are likely to behaved differently during aerosol dispersion. Although both MF and 450 M carriers produced low FPF, a higher FPF was observed in MF than the 450M. This was similar to a previous study where the FPF was higher from micronized carrier (carrier $d_{50\%}$ = 8.6 μm) than Lactochem (carrier $d_{50\%}$ = 20.1 μm) (Srichana et al., 1998).

The in vitro deposition studies conducted using all lactose samples clearly demonstrated that the presence of fine lactose in the mixture was important to achieve good dispersion of the salbutamol sulfate. However, for lactose carriers, like MF and 450 M, that possessed very high fractions of fine lactose, the dispersion

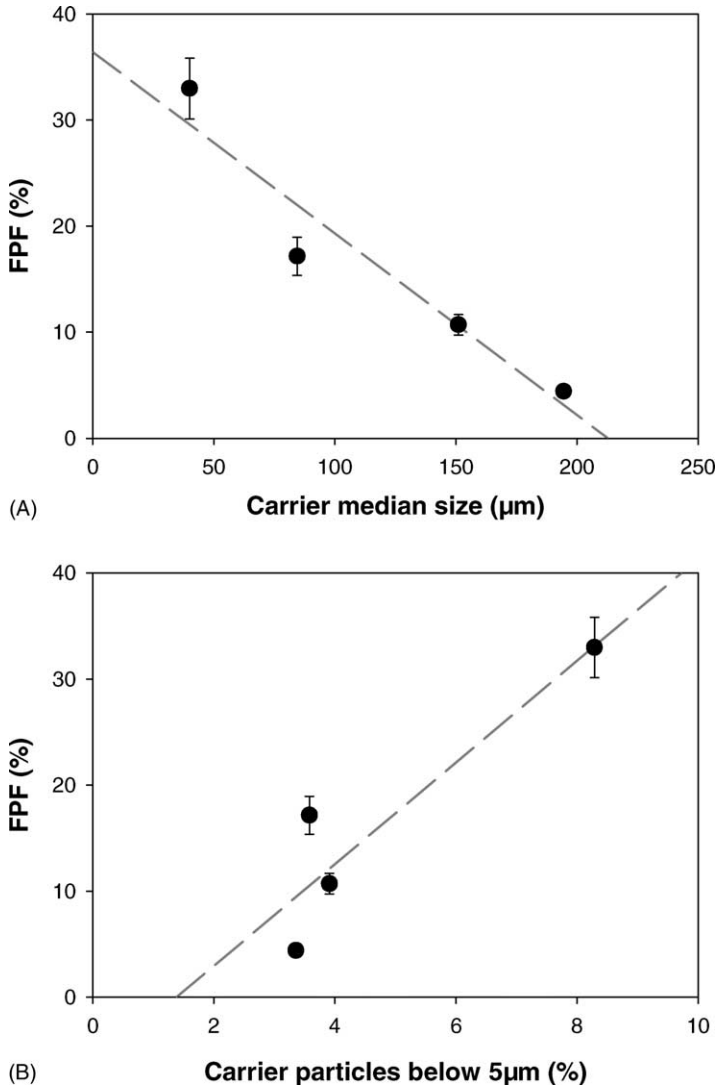

Fig. 4. Relationship between the FPF (mean ± S.D., $n = 5$) and (A) the carrier median diameter (regression coefficient, $r^2 = 0.92$) and (B) the proportion of carrier particles below 5 μm (regression coefficient, $r^2 = 0.81$) using sieved fractions of Edible lactose.

efficiency decreased. It seemed that the presence of both fine and large fractions of lactose were important for good dispersion. In order to test this, sieved fractions of the Edible carrier were added to micronized lactose (MF) and the dispersion efficiency of these SS (5%)-lactose mixtures determined. The presence of the larger fractions significantly affected the FPF ($P < 0.001$); the size fraction of the added lactose carrier did not significantly affect the FPF ($P = 0.195$) (Fig. 5). The FPF increased with increasing percentage of added large lactose carrier up to approximately 90%. Further increases caused a reduction in the FPF indicating that the presence of both large carrier particles and adhered micronized lactose were essential for increased drug dispersion. These results are consistent with the earlier studies which showed low FPF for the MF and 450 M carriers.

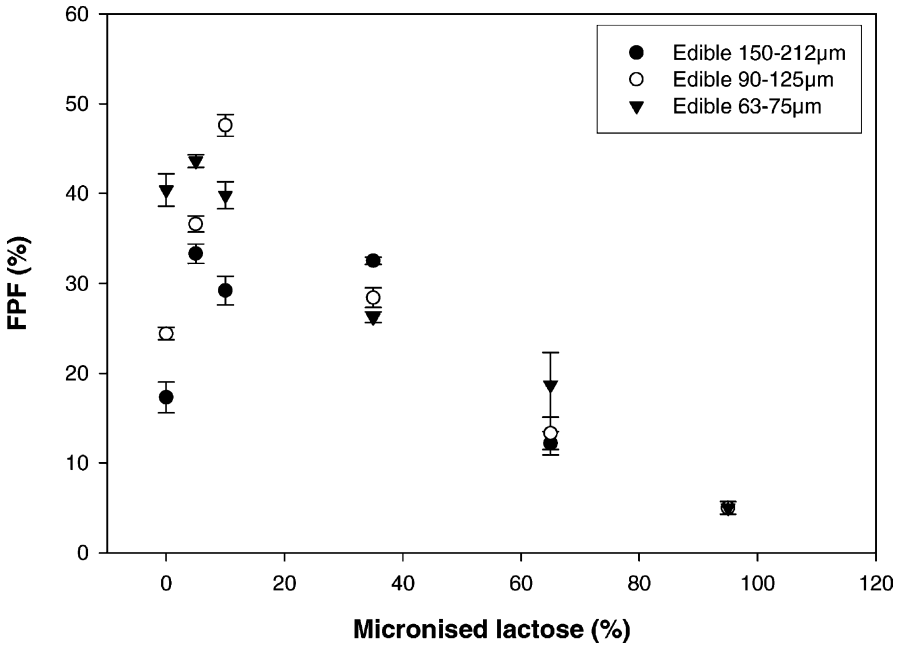

Fig. 5. Relationship between the FPF (mean ± S.D., $n = 5$) and the added proportion of micronized lactose (MF) to sieved fractions of Edible lactose.

4. Conclusion

Minimal differences were observed between these lactose samples when examined by XRD, DSC, TGA and vapor sorption. The differences in aerosol deposition of salbutamol sulfate from binary interactive mixtures containing lactose as the carrier could not be correlated to the solid state properties of the lactose used. Differences, observed between powder flow and adhesional properties of lactose carriers were also not correlated to the aerosol drug deposition. A correlation was demonstrated between FPF and median diameter of the carrier using all lactose carriers and sieved size fractions of Edible lactose carrier, except where a high proportion of fine carrier particles were present (e.g. MF and 450 M carriers). Closer examination showed correlation between FPF and the presence of fine carrier particles (e.g. particles less than 5 μm), demonstrating the importance of the fine adhered carrier particles in dispersion process. The improved dispersion, when lactose fines were associated with the carrier, was consistent with a proposed hypothesis relating to greater surface detachment and dispersion of mixed agglomerates of fine lactose and drug (Louey and Stewart, 2002). The existence of larger carrier particles was found to be essential to optimize the dispersion process, with maximum drug deposition achieved with carrier systems containing around 10% fine particle and 90% coarse particle concentrations. The influence of the coarse carrier on particle dispersion was only significant at fine particle concentrations up to about 10% in data collected, where the inherent adhered fine lactose particles were likely to become the dominant driver of the dispersion process. It is probable that the smaller carrier fractions possess higher concentrations of adhered fine lactose and that the inherent carrier size is less important in the dispersion process. This is shown clearly in Fig. 5, where there was no significant difference in FPF due to carrier size when there was an excess of fine particles (i.e. >35%). The reduction in FPF at high concentrations of fine particles was consistent with our initial results and could be related to the dilution of drug in the agglomerates as the fine lactose is added. Using estimates of number of particles per unit weight of mixture based on SS and micronized lactose diameters of 1.3 and 4 μm, the ratio of SS to lactose reduced from 15:1 to 1.5:1 as the added micronized lactose content of the

mixture increased from 10 to 95%. Lack of mechanical disruption of agglomerates by the large carrier particles may also contribute to the trends seen in the study. The results obtained in this study are obtained from powder mixtures prepared on a laboratory scale and care should be taken in extending the interpretations to full scale processing where mixing energies may be different.

Acknowledgements

MDL was supported by a Monash University Graduate Scholarship

References

Alway, B., Sangchantra, R., Stewart, P.J., 1996. Modelling the dissolution of diazepam in lactose interactive mixtures. Int. J. Pharm. 130, 213–224.

Angberg, M., Nyström, C., Castensson, S., 1991. Evaluation of heat-conduction microcalorimetry in pharmaceutical stability studies. III. crystallographic changes due to water vapour uptake in anhydrous lactose powder. Int. J. Pharm. 73, 209–220.

Braun, M.A., Oschmann, R., Schmidt, P.C., 1996. Influence of excipients and storage humidity on the deposition of disodium cromoglycate (DSCG) in the twin impinger. Int. J. Pharm. 135, 53–62.

Buckton, G., Darcy, P., 1995. The use of gravimetric studies to assess the degree of crystallinity of predominantly crystalline powders. Int. J. Pharm. 123, 265–271.

Byron, P.R., 1986. Some future perspective for unit dose inhalation aerosols. Drug Dev. Ind. Pharm. 12, 993–1015.

Byron, P.R., Kelly, E.L., Kontny, M.J., 1994. Recommendations of the USP Advisory Panel on aerosols on the USP general chapters on aerosols <601> and uniformity of dosage units <905>. Pharm. Forum 20, 7477–7505.

Chan, H.-K., Clark, A., Gonda, I., Mumenthaler, M., Hsu, C., 1997. Spray dried powders and powder blends of recombinant human deoxyribonuclease (rhDNase) for aerosol delivery. Pharm. Res. 14, 431–437.

Crooks, M.J., Ho, R., 1976. Ordered mixing in direct compression of tablets. Powder Technol. 14, 161–167.

French, D.L., Edwards, D.A., Niven, R.W., 1996. The influence of formulation on emission, deaggregation and deposition of dry powder for inhalation. J. Aerosol Sci. 27, 769–783.

Ganderton, D., 1992. The generation of respirable clouds from coarse powder aggregates. J. Biopharm. Sci. 3, 101–105.

Hersey, J.A., 1975. Ordered mixing: a new concept in powder mixing practice. Powder Technol. 11, 41–44.

Kassem, N.M., Ho, K.K.L., Ganderton, D., 1989. The effect of air flow and carrier size on the characteristics of an inspirable cloud. J. Pharm. Pharmacol. 41, 14P.

Kassem, N.M., Ganderton, D., 1990. The influence of carrier surface on the characteristics of inspirable powder aerosols. J. Pharm. Pharmacol. 42, 11P.

Kawashima, Y., Serigano, T., Hino, T., Yamamoto, H., Takeuch, H., 1998. Effect of surface morphology of carrier lactose on dry powder inhalation property of pranlukast hydrate. Int. J. Pharm. 172, 179–188.

Kibbe, A.H. (Ed.), 2000. Handbook of Pharmaceutical Excipients, 3rd ed. London Pharmaceutical Press, London, pp. 276–285.

Lerk, C.F., Andreae, A.C., de Boer, A.H., de Hoog, P., Kussendrager, K., van Leverink, J., 1984. Alteration of α-lactose during differential scanning calorimetry. J. Pharm. Sci. 73, 856–857.

Louey, M.D., Mulvaney, P., Stewart, P.J., 2001. Characterisation of adhesional properties of lactose carriers using atomic force microscopy. J. Pharm. Biomed. Anal. 25, 559–567.

Louey, M.D., Stewart, P.J., 2002. Particle interactions involved in aerosol dispersion of ternary interactive mixtures. Pharm. Res. 19, 1524–1531.

Mackin, L.A., Rowley, G., Fletcher, E.J., 1997. An investigation of carrier particle type, electrostatic charge and relative humidity on in vitro drug deposition from dry powder inhaler formulations. Pharm. Sci. 3, 583–586.

Neumann, B.S., 1967. The flow properties of powders. In: Bean, H.S., Carless, J.E., Beckett, A.H. (Eds.), Advances in Pharmaceutical Science. Academic Press, New York, pp. 181–221.

Podczeck, F., 1998. The relationship between physical properties of lactose monohydrate and the aerodynamic behaviour of adhered drug particles. Int. J. Pharm. 160, 119–130.

Sebhatu, T., Elamin, A.A., Ahlneck, C., 1994. Effect of moisture sorption on tabletting characteristics of spray dried (15% amorphous) lactose. Pharm. Res. 11, 1233–1238.

Srichana, T., Martin, G.P., Marriott, C., 1998. On the relationship between drug and carrier deposition from dry powder inhalers in vitro. Int. J. Pharm. 167, 13–23.

Staniforth, J.N., 1988. Powder flow. In: Aulton, M.E. (Ed.), Pharmaceutics: The Science of Dosage Form Design. Churchill Livingstone, New York, pp. 600–615.

Steckel, H., Müller, B.W., 1997. In vitro evaluation of dry powder inhalers II: influence of carrier particle size and concentration on in vitro deposition. Int. J. Pharm. 154, 31–37.